Control
and Cybernetics

VOL. 18 (1989) No. 2

Mathematical modelling of gas-solid reactions in a class of fluidized bed coal gasifiers

by

ANTONI ŻOCHOWSKI

Systems Research Institute
Polish Academy of Sciences
Newelska 6
01-447 Warsaw, POLAND

A general model of gas-solid reactions in fluidized bed reactor presented in [8] is applied to coal gasification process. Numerical schemes and results of computations are presented for averaged isothermal and distributed isothermal models. Results are checked against laboratory measurements reported in [7].

KEY WORDS: reaction-diffussion systems, gas-solid reactions, coal gasification.

1. Introduction

The following paper represents a continuation of [8], where a model of gas-solid reactions in fluidized reactors has been propesed. Here we apply the model of [8] to a coal gasifier fed by pure high-temperature steam.

Since the physical processes taking place in the fluidized bed have already been described in [8], here we shall only recall their final mathematical form. The chemical part of the model will be presented in more detail.

As it is mentioned in [8], the full model of a reactor may be simplified in three ways: by space averaging, transition to stationary state and/or neglecting thermal effects. In this paper we consider two of these cases:

— averaged isothermal model,
— distributed isothermal model.

The data for numerical experiments originate from [7], where one can also find the results of measurements in laboratory installation. These results provide at least partial validation of the models used.

2. The model of steam-fed coal gasification reactor

2.1. A full isothermal model

Let us recall that the reactor consists of a vessel containing the fluidized bed together with
— fluidizing gas (steam) distributor,
— a feeder for injecting coal powder,
— a gas outlet,
— an outlet for removing partially reacted coal particles.
In the bed one can discern two phases, the emulsion being the mixture of a gas with solid particles and the bubble phase containing only gases. Structure of such reactor is schematically shown in Fig. 1, together with location of coordinate axis used throughout the paper. In the model the following gaseous components are taken into account (numbers refer to the corresponding indices)

$$1-CO \qquad 2-CO_2 \qquad 3-H_2 \qquad 4-H_2O \qquad 5-CH_2$$

The bubble phase is distinguished by the superscript h, the emulsion phase by e.

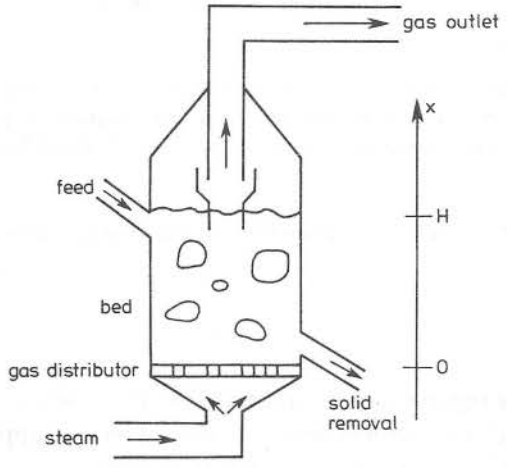

Fig.1. A fluidized bed gasifier

Among the reactions taking place in the bed the following five are considered to dominate the process, [7], [13]:

$$C+H_2O \xrightarrow{k_1} CO+H_2$$

$$C+CO_2 \xrightarrow{k_2} 2CO$$

$$C+2H_2 \xrightarrow{k_3} CH_4$$

$$CO+H_2O \xrightarrow{k_4} CO_2+H_2$$

$$CO+H_2O \xleftarrow{k_5} CO_2+H_2$$

It is assumed that no devolatisation or cracking occur in the reactor, i.e. it is fed with pure coal particles or the injected particles have been devolatilised previously.

Kinetics of the chemical reactions is characterised in the usual Arrhenius form

$$k_i(T) = k_i^0 \exp(-E_i / RT). \tag{1}$$

In the emulsion phase all the above reactions take place simultaneously, while in bubble phase we have to do with reactions 4 and 5 only. Let us denote R_i^b, R_i^e the intensities of generation for appropriate gases. Then we have:

— for bubble phase:

$$\begin{gathered} R_1^b = R_1^b = -R^b \\ R_2^b = R_3^b = R^b \\ R_5^b = 0, \end{gathered} \tag{2}$$

where

$$R^b = k_4 C_1^b C_4^b - k_5 C_2^b C_3^b.$$

— for emulsion phase:

$$\begin{gathered} R_1^e = S(k_1 C_4^e + \frac{1}{2} k_2 C_2^e) - R^e, \\ R_2^e = -S k_2 C_2^e + R^e, \\ R_3^e = S(k_1 C_4^e - k_3 C_3^e) + R^e, \\ R_4^e = -S k_1 C_4^e - R^e, \\ R_5^e = \frac{1}{2} S k_3 C_3^e, \end{gathered} \tag{3}$$

where

$$R^e = k_4 C_1^e C_4^e - k_5 C_2^e C_3^e.$$

The active surface of coal particles unit volume of emulsion phase may be expressed as

$$S = A_C \frac{W_C}{HA(1-\delta)}, \tag{4}$$

where W_C — mass of the coal in the bed, and A_C — active surface of the coal per unit weight.

Ac is determined by the statistical distribution of coal particle sizes.

The last equation of the model describes the rate of coal consumption and has the form

$$R_C = -W_C A_C M_C (k_1 C_4^e + k_2 C_2^e + \frac{1}{2} k_3 C_3^e, \tag{5}$$

Since the model we are considering is isothermal, this completes the description of its chemical part. It should be stressed here that in order to derive the above formulae it was neccessary to make many simplifications concerning e.g the orders of reactions, the number of reactions taking place etc.: for more detailed discussion see [13].

The hydrodynamical part has been specified in [8] in detail. Here we only recall that the bed height H is computed by solving some nonlinear algebraic equation involving working parameters of the reactor, which may be written symbolically as

$$\Phi(H; u_0, u_{mf}, \varepsilon_{mf}, W, A, \bar{\rho}) = 0 \tag{6}$$

Having H, one can obtain the fraction δ denoting the volume share of bubble phase,

$$\delta = \delta(H, u_0, u_{mf}). \tag{7}$$

After fixing H, we may formulate advection-diffusion equations describing the behaviour of gaseous components:

$$\frac{\partial C_i^b}{\partial t} = -u^b \frac{\partial C_i^b}{\partial x} + D_i^b \frac{\partial^2 C_i^b}{\partial x^2} - F_{be}(C_i^b - C_i^b) + R_i^b,$$

$$\frac{\partial C_i^e}{\partial t} = -\frac{u^e}{\varepsilon_{mf}} \frac{\partial C_i^e}{\partial x} + \frac{D_i^e}{\varepsilon_{mf}} \frac{\partial^2 C_i^e}{\partial x^2} + \frac{\delta}{1-\delta} \frac{F_{be}}{\varepsilon_{mf}} (C_i^b - C_i^b) + \frac{R_i^e}{\varepsilon_{mf}}, \tag{8}$$

$$x \in (0, H), \quad t > 0, \quad i = 1,...,5$$

with boundary conditions:

$$x = 0: \qquad C_i^b - \frac{D_i^b}{u^b} \frac{\partial C_i^b}{\partial x} = C_{i0},$$

$$C_i^e - \frac{D_i^e}{u^e} \frac{\partial C_i^b}{\partial x} = C_{i0}, \; i = 1,...,5 \tag{9}$$

$$x = H: \qquad \frac{\partial C_i^b}{\partial x} = 0,$$

$$\frac{\partial C_i^e}{\partial x} = 0, \quad i = 1,...,5$$

and initial conditions for $t = 0$:

$$C_i^b = C_i^e = C_{i0}, \; i = 1,...,5.$$

Similarly to gases, the mass of the coal contained in the bed has a dynamics described by the equation

$$\frac{dW_C}{dt} = W_{in} - \frac{W_C}{W} W_{out} - R_C. \tag{10}$$

subject to initial condition $W_C(0) = W_{C0}$.

2.2. Working regime

As it is evident from (6), the height of the fluidized bed depends strongly on the mass of solids. Equations (8) have been written under the assumption that $H = const.$, so thay may be applied only to the working regime in which the mass W is also kept constant. The only practical way to achive this is by using intensities of feeding (or removal) as control variables. Therefore we assume that the control system of reactor contains some sensors measuring the bed height, influencing via actuators the feeding rate. The rate of removal is assumed fixed. The sketch of such an installation is given in Fig.2.

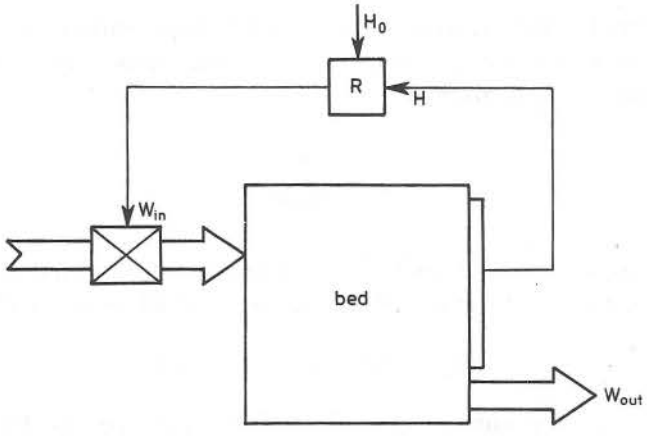

Fig.2. The control of reactor

The overall aim of such a control system is to stabilise H at some value H_0. The dynamics of H is neglected in this model. Such simplification allows us to determine the evolution of coal mass in the bed explicitly. Let us notice that the mass of the whole bed fulfils the equation:

$$\frac{dW}{dt} = W_{in} - W_{out} - R_C. \tag{11}$$

Since $W = const$, one obtains

$$W_{in} - R_C = W_{out}.$$

After substitution into (10), the coal mass W_C satisfies the problem

$$\frac{dW_C}{dt} = W_{out} - \frac{W_{out}}{W} W_C, \tag{12}$$

$$W_C(0) = W_{C0}.$$

Equation (12) may be easily integrated, giving:

$$W_C = W(1 - e^{-\beta t}) + W_{C0e}{}^{-\beta t}, \tag{13}$$

$$\beta = W_{out} / W.$$

Even if initially the bed contains neutral particles, i.e. $W_{C0} \neq W$, after some time they are replaced and $W_C \to W$ as $t \to \infty$.

2.3. Evolution of particle population

Let us recall briefly main features of the particle population model given in [8]. The bed contains spherical coal particles with radii satisfying $r \in (0, r_{max})$. The normalising factor N_0 is given by

$$N_0 = \frac{6W}{\Pi \rho r^3{}_{max}}. \tag{14}$$

The particle population is described by means of a normalised distribution of quantities of particles as function of radius, $n(r, t)$, which must satisfy a condition

$$N_0 \int_0^{r\,max} \mathrm{n}(r, t)\, dr = N_C(t),$$

where $N_C(t)$ — a total number of coal particles in the bed at the moment t.

The particles are being consumed while staying in reactor and the rate of shrinking is given as (see (5)):

$$v = M_C(k_1 C_4^e + k_2 C_2^e + \frac{1}{2} k_3 C_3^e) / \rho \tag{15}$$

The assumption that $W = const.$ allows us to compute the feeding intensity, see (11):

$$W_{in}(t) = 4 \Pi \rho v N_0 \int_0^{r_{max}} n(r, t) r^2\, dr + W_{out}. \tag{16}$$

Also the active surface of coal per unit volume of emulsion phase is easily obtained,

$$S(t) = \frac{4\Pi N_0}{HA(1-\delta)} \int_0^{r_{max}} n(r, t) r^2 \, dr. \tag{17}$$

The complete model of particle population evolution takes on the form:

$$\frac{\partial n}{\partial t} = v\frac{\partial n}{\partial r} - \frac{W_{out}}{W} n + \frac{3W_{in}}{4\Pi\rho r^3 N_0} p^{in}(r), \tag{18}$$

$$n(r, 0) = n_0(r), r \in (0, r_{max}),$$

with addition of equations (15) and (16).

Relationships (15) and (17) link equation (18) with the dynamics of gas components.

3. The averaged model

3.1. Formal description

The averaged isothermal model results from integration of advection-diffusion equations with respect to x over the interval $(0, H)$. Let the operator of averaging be defined as

$$\overline{(\bullet)} = \frac{1}{H} \int_0^H (\bullet)\, dx \tag{19}$$

The right-hand sides expressions R_i^b, R_i^e depend nonlinearly on concentrations, so they cannot be averaged directly. They are approximated by $\bar{R}_i^b$, $\bar{R}_i^e$ obtained by replacing original functions $C_i^b(r, t)$, $C_i^e(x, t)$ with averaged values $\bar{C}_i^b(t)$, $\bar{C}_i^e(t)$. The new expressions are denoted $\bar{R}_i^b(t)$, $\bar{R}_i^e(t)$. After taking into account boundary conditions (9) one obtains from (8) the system of ordinary differential equations

$$\frac{d\bar{C}_i^b}{dt} = \bar{R}_i^b - \left(F_{be} + \frac{1}{H}u_b\right)\bar{C}_i^b + F_{be}\,\bar{C}_i^e + \frac{1}{H}u_b\Big) C_{i0},$$

$$\frac{d\bar{C}_i^e}{dt} = \frac{1}{\varepsilon_{mf}}\bar{R}_i^e - \frac{1}{\varepsilon_{mf}}\left(\frac{\delta}{1-\delta}F_{be} + \frac{1}{H}u_e\right)\bar{C}_i^e + \frac{1}{\varepsilon_{mf}}\frac{\delta}{1-\delta}F_b^e\,\bar{C}_i^b \tag{20}$$

$$+ \frac{1}{H\varepsilon_{mf}}u_e C_{i0},$$

$$\bar{C}_i^b(0) = \bar{C}_i^e(0),\ i = 1,\ldots,5.$$

The above equations are supplemented with the equation of particles evolution (18) and relations (15), (17). Since the bed height H may be computed only once before the start of the model, and then stays constant, we assume it to be a parameter.

The final form of a isothermal averaged model may be summarised as:

$$\frac{d\bar{C}}{dt} = \tilde{f}_1(\tilde{C}, n),$$

$$\frac{\partial n}{\partial t} = v(\tilde{C})\frac{\partial n}{\partial r} + f_2(\tilde{C}, n), \tag{21}$$

with initial conditions

$$\tilde{C}(0) = \tilde{C}_0, n(r, 0) = n_0(r), \; r \in (0, r_{max}).$$

Here

$$\tilde{C}(t) = (\tilde{C}_1^b(t), \tilde{C}_1^e(t), \ldots, \tilde{C}_5^b(t), C_5^e(t))^T,$$

$$\tilde{C}_0 = (C_{10}, C_{10}, \ldots, C_{50}, C_{50})^T$$

3.2. Solution method

In the process of solving (21) every time step splits into two stages. In the first stage a new value of $\tilde{C}$ is computed, for fixed $n(r, t)$. Then, using a new vector $\tilde{C}$, the coefficients of transport equation describing evolution of n are calculated. Finally, a new value of n is obtained. Such solution strategy implied that onestep algorithms had to be used for ordinary differential equations as well as for the transport equation.

For the system of ordinary differential equations the predictor-corrector method with additional correction to convergence has been applied. It is known, [11], that such method is unconditionally stable and equivalent to implicit scheme. It may be symbolically written down for a given time step dt in the following form:

(i) perform twice the predictor-corrector operation

$$\tilde{C}^*_{t+1/3} := \tilde{C}_t + \tilde{f}_1(\tilde{C}_t, n_t)dt,$$

$$\tilde{C}^*_{t+2/3} := \tilde{C}_t + \frac{1}{2}[\tilde{f}_1(\tilde{C}_t, n_t) + \tilde{f}_1(\tilde{C}^*_{t+1/3}, n_t)]\,dt,$$

$$\tilde{C}^*_{t+1} := \tilde{C}_t + \frac{1}{2}[\tilde{f}_1(\tilde{C}_t, n_t) + \tilde{f}_1(\tilde{C}^*_{t+2/3}, n_t)]\,dt \tag{22}$$

$$d\tilde{C}^* := \tilde{C}^*_{t+1} - \tilde{C}_t.$$

(ii) repeat correction to convergence using Newton method for $d\tilde{C}^*$:

$$\tilde{e} := \frac{1}{2}[\tilde{f}_1(\tilde{C}_t) + \tilde{f}_1(\tilde{C}_t + d\tilde{C}^*)]\,dt - d\tilde{C}^*,$$

$$A := \frac{1}{2}d\tilde{f}_1\,dt - I, \tag{23}$$

$$\tilde{r} := A^{-1}\tilde{e},$$

$$d\tilde{C}^* := d\tilde{C}^* - \tilde{r},$$

$$\text{until } \|\tilde{e}\| < \varepsilon.$$

(iii) compute corrected values:

$$\tilde{C}_{t+1} := \tilde{C}_t + d\tilde{C}^*.$$

Here I denotes the unit matrix, and $d\tilde{f}_1$ — jacobian of f_1 with respect to $\tilde{C}_1$.

In principle, the step (i) alone guarantees the stabillity for the second order Adams-type method, [11]. Additional corrections (ii) do not change stability properties, but diminish the solution error. Matrices A and A^{-1} are renewed only sporadically, when the iteration count in step (ii) exceeds certain given value, so their presence does not add much to the computation time.

The transport equation for $n(r, t)$ is solved by means of an implicit second order difference scheme, using the method of characteristics. The family of characteristics for such equation consists of curves $R = R(t)$ satisfying

$$\frac{dR}{dt} = -v \tag{24}$$

The method of characteristics is based on introducing a new function

$$n_R(t) = n(R(t), t). \tag{25}$$

The total time derivative of such function fulfils the relation

$$\frac{Dn_R}{Dt} = -v\frac{\partial n}{\partial r} + \frac{\partial n}{\partial t},$$

and hence

$$\frac{Dn_R}{Dt} = f_2(\tilde{C}, n(R(t), t)). \tag{26}$$

The implicit second order difference scheme has been applied to (26) giving

$$n_R(t + dt) - n_R(t) = \frac{1}{2}[f_2|_{t+dt} + f_2|_t]\,dt. \tag{27}$$

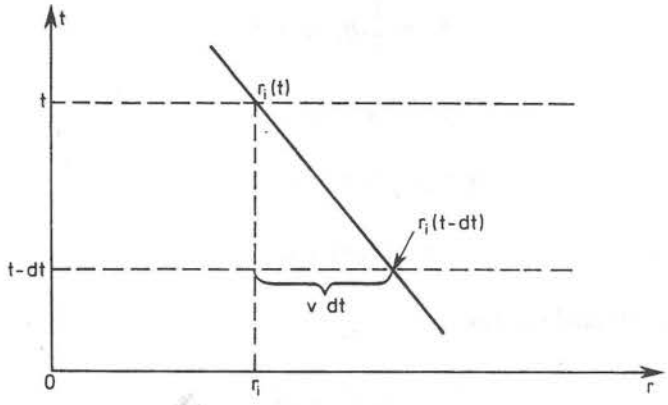

Fig.3. Characteristics for transport equation

Let us now introduce a discretisation of the interval $[0, r_{\max}]$, see Fig. 3. Let $r_i(t)$ be a curve satisfying (24) and crossing through point (r_i, t). Denote

$$n_i(t) = n(r_i(t), t), \tag{28}$$

and apply the scheme (27) to $n_i(t)$:

$$n(r_i(t), t) - n(r_i(t - dt), t - dt) =$$

$$\frac{1}{2}[f_2(\tilde{C}, n(r_i(t), t)) + f_2(\tilde{C}, n(r_i(t - dt), t - dt))]\,dt$$

Since

$$r_i(t - dt) \approx r_i + v\,dt,$$

the final difference equation has the form:

$$n(r_i(t), t) = n(r_i + v\,dt, t - dt) +$$

$$+ \frac{1}{2}[f_2(\tilde{C}, n(r_i(t), t)) + f_2(\tilde{C}, n(r_i + v\,dt, t - dt))]\,dt, \tag{29}$$

$$i = 1, \ldots, k.$$

In case when $r_i + v\,dt > r_{\max}$ it was assumed that $n\,(r_i + v\,dt,\ t - dt) \equiv 0$. Such an assumption allowed us to limit solution to the interval $[0, r_{\max}]$, in spite of the fact that in principle the transport equation is defined on the whole axis $r \in (-\infty, \infty)$.

Both methods described above were independently tested on known examples, especially with respect to their stability.

3.3. Simulation results

The numerical experiments have been performed for the reactor and conditions identical as in [7]. In this way there was a possibility to compare the results with experimental data. There is, however, an important difference. In [7] the coal particles were porous with active surface $A_C = 200000\,m^2/kg$, much bigger than that corresponding to smooth spherical particles. It was compensated for by increasing reactions frequency factors in such a way, that a powder consisting of spheres with uniform radii $r = \frac{1}{2} r_{max}$ reacted with the same intensity as porous particles. Such adjustement amounts to assuming that the active surface of porous particles is proportional to their outer surface, which is a rather rough approximation.

For values of chemical parameters we refer the reader to [7]. The structural and working parameters of the experimental installation were as follows (for the meaning and units see Notation):

$D = 0.1$, $W = 0.973$, $u_{mf} = 0.1$, $\varepsilon_{mf} = 0.43$, $D_i^b = 0.001$,
$D_i^c = 1000$, $T = 1000$, $u_0 = 0.165$, $W_{out} = 0.1$, $C_{40} = 100\%\ H_2O$,
$r_{max} = 0.0003$.

The adjustement factor for k_i, $i = 1, 2, 3$, resulting from the value of r_{max} given above was $2.5 \cdot 10^4$. The feeding powder consisted of particles with uniform radii

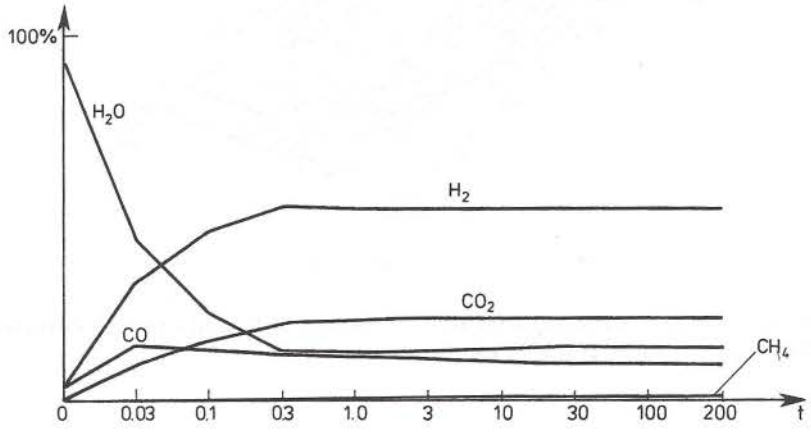

Fig.4. Composition of the outgoing gas

equal 0,9 r_{max}. For the discretisation of (29) the interval [0, r_{max}] has been divided into 20 parts, while time step was variable.

Two numerical experiments have been performed:

1⁰ At the start of simulation the bed contains only neutral particles. The processes are comparativley slow and a steady state is reached after about 200 s.

2⁰ The bed initially contains coal consisting of particles with uniform radii $\frac{1}{2} r_{max}$.

The processes are more abrupt, there are even traces of oscillations. The time of reaching a steady state is similar. Since this is a more interesting case, the history of concentrations for the outgoing gas are given in Fig.4, together with evolution of particle sizes distribution, Fig.5. A quasi logarithmic time scale is used, in order to give better resolution of fast initial phase.

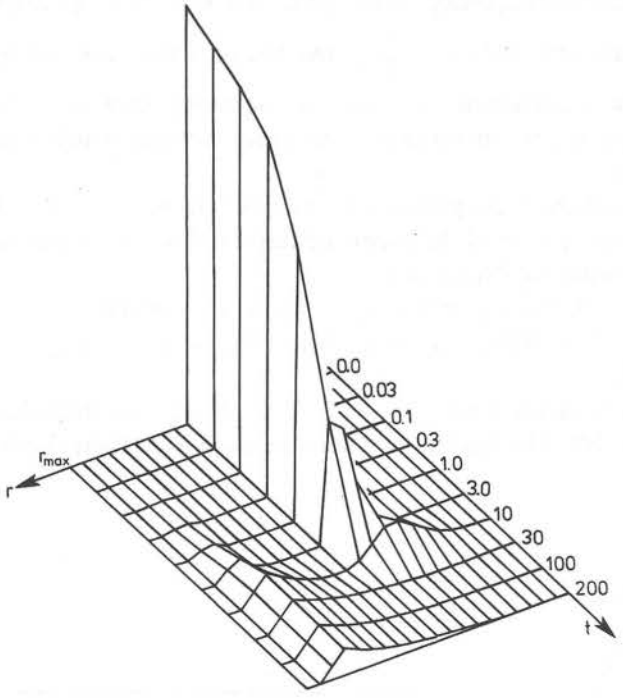

Fig.5. Evolution of particles

The steady state concentrations are very similar for both cases. A comparison with [7] will be given in the last section.

4. Distributed isothermal model

4.1. Formal description

Let us notice that couplings between individual equations in system (8) enter only terms responsible for mass transfer through the interface between emulsion phase and bubble phase and in the righ-hand sides describing chemical reactions. Diffusion and advection processes are autonomous for each component. Hence (8) may be written in the form of the following nonlinear parabolic system:

$$\frac{\partial C_i}{\partial t} + u_i \frac{\partial C_i}{\partial x} - D_i \frac{\partial^2 C_i}{\partial x^2} = g_i(\tilde{C}, n), \tag{30}$$

with boundary conditions:

$$\begin{aligned} x = 0: &\qquad u_i c_i - D_i \frac{\partial C_i}{\partial x} = u_i C_{i0} \\ x = H: &\qquad \frac{\partial C_i}{\partial x} = 0, \end{aligned} \tag{31}$$

$$t = 0 : \mathrm{C}_i(x, 0) = C_{i0},\ x \in [0, H],$$

$$i = 1,2,...,10.$$

Here $C_{2i-1} = C_i^b$, $C_{2i} = C_i^f$ and similarly for u_i, D_i, see (8).

To complete the model, one must of course extend it with particle population dynamics (18).

4.2. Solution method

A specific form of the system (30) suggests convenience of solving it by so-called splitting into physical processes. Let us denote by L_i a differential operator

$$L_i(C_i) = D_i \frac{\partial^2 C_i}{\partial x^2} - u_i \frac{\partial C_i}{\partial x}, \qquad i = 1,...,10.$$

Then (30) may be discretised with respect to time in the following way:

$$\frac{C_i^*(t + dt) - C_i(t)}{dt} = g_i(\tilde{C}(t), n),$$

$$C_i^{**}(t) = C_i^{*}(t + dt), \tag{32}$$

$$\frac{C_i(t + dt) - C_i^{**}(t)}{dt} = L_i(C_i^{**}(t), n),\ i = 1,...,10.$$

Adding the above equations gives the relation

$$\frac{C_i(t + dt) - C_i(t)}{dt} = g_i(\tilde{C}(t), n) + L_i(C_i^{**}(t), n).$$

Let us note that if functions g_i are smooth enough, convergence

$$L_i\,(C_i^{**}\,(t),\, n) \to L_i\,(C_i\,(t),\, n),$$

as $dt \to 0$ is ensured. It means that the system (32) is asymptotically equivalent to (30) and may be therefore used as its approximation.

Solving the first of equations (32) consists in making one time step from t to $t + dt$ for

$$\frac{dC_i^{*}}{dt} = g_i(\tilde{C},\, n),\ i = 1,...,10, \tag{33}$$

with initial conditions

$$C_i^{*}\,(t) = C_i\,(t).$$

The algorithm for such problem has already been introduced in Section 3.2.

The second part of the system (32) may be treated as realisation of time step from t to $t + dt$ for equation

$$\frac{\partial C_i}{\partial t} = L_i(\tilde{C}_i,\, n),\ i = 1,...,10, \tag{34}$$

with initial conditions

$$C_i\,(t) = C_i^{**}\,(t), \quad i = 1,...,\,10.$$

Equations in (34) are independent of each other and have the form

$$\frac{\partial C}{\partial t} + u\frac{\partial C}{\partial x} - D\frac{\partial^2 C}{\partial x^2} = 0, \tag{35}$$

with boundary conditions

$$x = 0: \qquad uc - D\frac{\partial C}{\partial x} = uC_0,$$

$$x = H: \qquad \frac{\partial C}{\partial x} = 0, \tag{36}$$

For solving (35), (36) we shall use the finite difference method. Let us divide the interval $[0, H]$ into l parts,

$$0 = x_1 < x_2 < \ldots < x_{i+1}\, H, |x_{i+1}\, x_i| = h.$$

Then we approximate the equation (35) by means of an unconditionally stable difference scheme [6], using notation $C(i, k) = C(i \cdot h, k \cdot dt)$:

$$C(i, k+1) - C(i, k) + \frac{u \cdot dt}{h}[C(i, k+1) - C(i-1, k+1)] +$$

$$- \frac{D \cdot dt}{h^2}[C(i-1, k+1) - 2C(i, k+1) + C(i+1, k+1)] = 0. \tag{37}$$

for $1 < i < l + 1$. After introducing notations

$$a = u \cdot dt/h,$$

$$b = D \cdot dt/h^2,$$

the system (37) reduces to

$$-(a+b)\, C(i-1, k+1) + (1+a+2b)\, C(i, k+1) - bC(i+1, k+1)$$

$$= C(i, k),$$

$$1 < i < l+1. \tag{38}$$

The first and last equations require taking into account the boundary conditions (36), what leads to

$$(1+a+b)\, C(1, k+1) - bC(2, k+1) = C(1, k) + aC_0$$

$$-(a+b)\, C(l, k+1) + (1+a+b)\, C(l+1, k+1) = C(l+1, k) \tag{39}$$

As a result, from (38) and (39) one obtains a symmetric, positive definite tridiagonal linear system

$$A\tilde{C}(k+1) = \tilde{C}(k) + a\tilde{C}_0, \tag{40}$$

where $\tilde{C}(*) = (C_1(1, *),..., C(l+1, *))^T$, and $\tilde{C}_0 = (C_0\ 0,..., 0)^T$. Such system may be very effectively solved using for example Cholesky decomposition.

In its final form the algorithm for distributed model may be outlined as follows:

— for each point x_i, $i = 1,..., l+1$ solve the system of ordinary differential equations (33) in $(t, t+1)$,

— after taking the results of the former step as an initial condition solve the advection-diffussion equations (34),

— solve the equation of particle population dynamics (21).

4.3. Simulation results

All the data for numerical experiments performed with distributed model were the same as in the case of the averaged one, described in Section 3.3. The interval $[0, H]$ has been divided, for the discretisation of the advection-diffussion

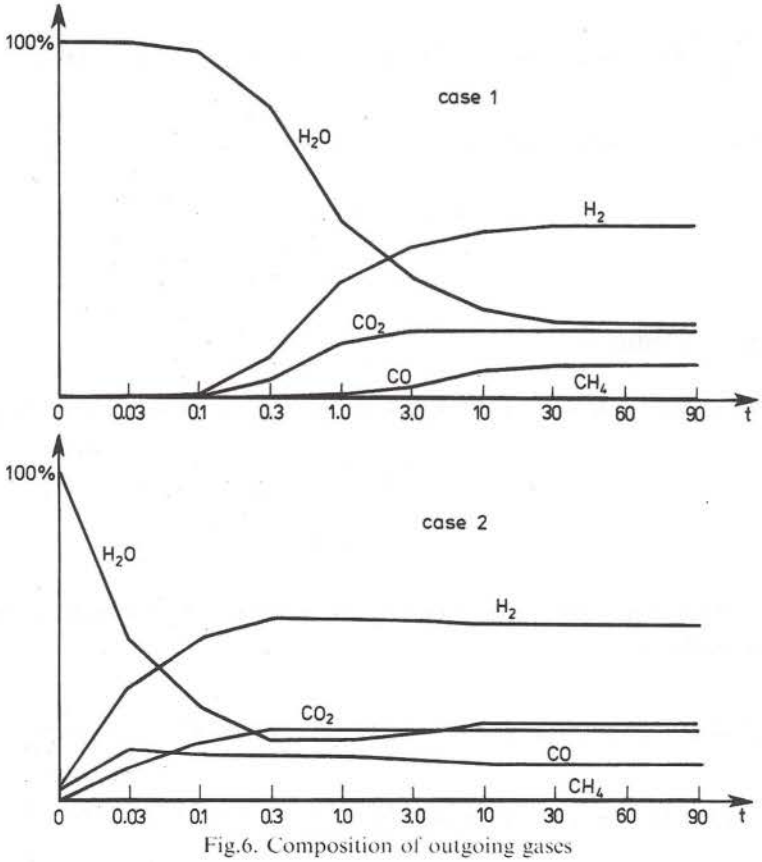

Fig.6. Composition of outgoing gases

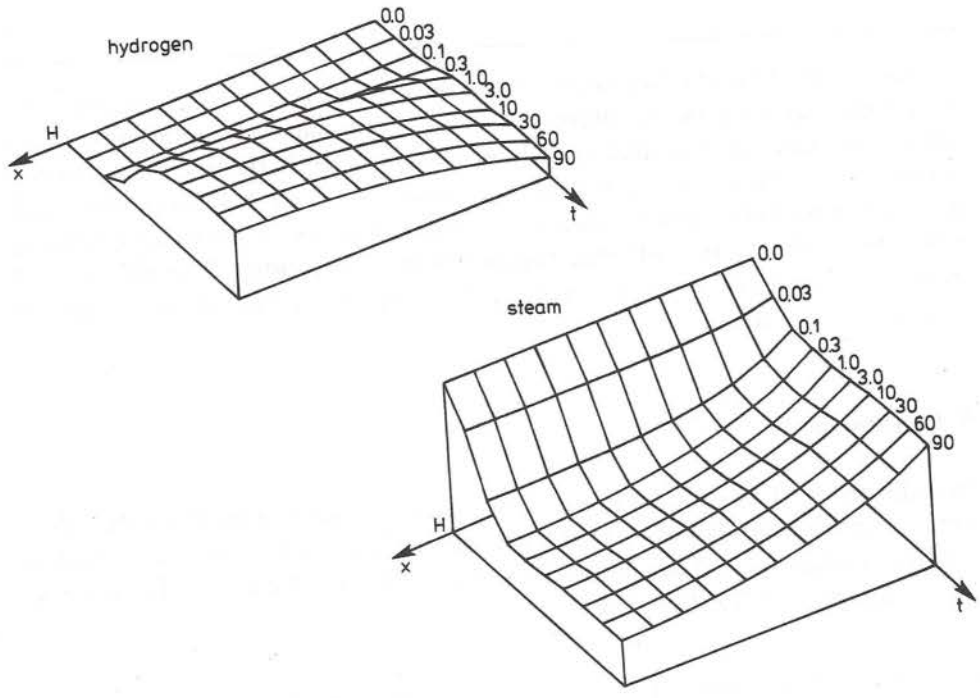

Fig. 7. Evolution of concentrations case 1

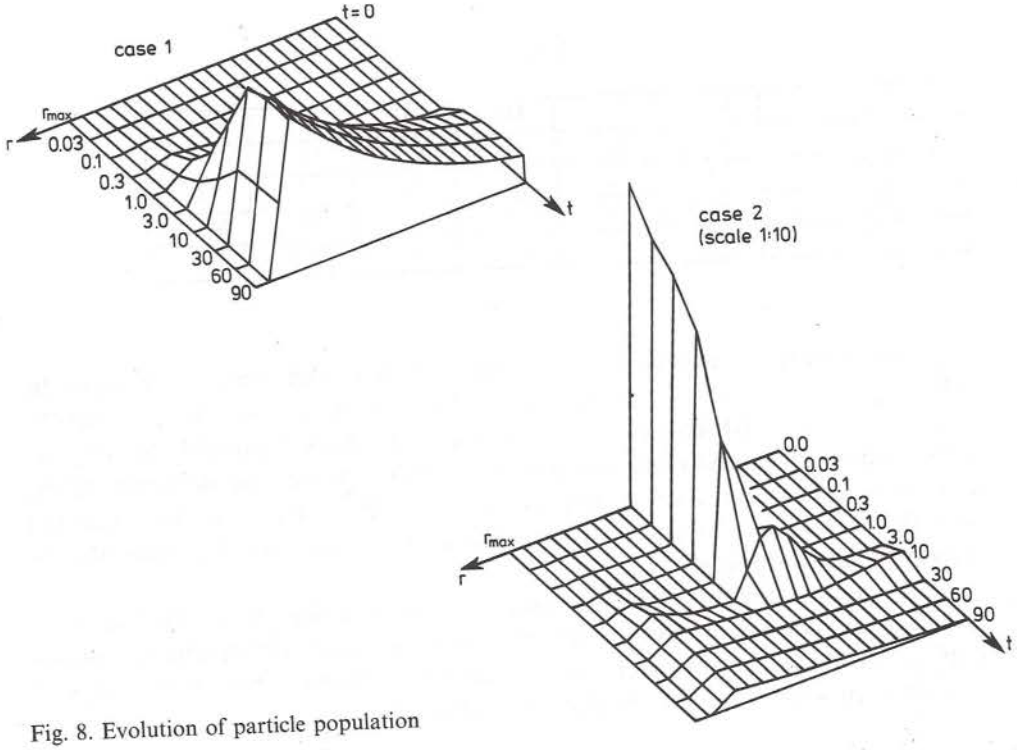

Fig. 8. Evolution of particle population

equation, into 10 parts. Because of the long computation time, the sequence of time moments used in the presentation of results has been shortened. Two simulation runs were executed, exactly as in Section 3.3. In the first the initial bed contens was neutral, in the second it consists of uniform spheres with radii $0.5r_{max}$. Fig.6 shows the compositions of outgoing gases for both cases, while in Fig.7 the evolution of hydrogen concentration is presented. The influence of initial bed reactivity is clearly visible. Fig.8 gives a comparison of particle population evolutions.

5. Conclusions

In order to check the results given by the models described in this paper, they were compared with laboratory results given in [7], as well as the mathematical model described there. The composition of gases leaving the reactor in each case are summarised in Table 1. Here

I — chemical experiment [7],
II — lumped model [7],
III — averaged model, case 1,
IV — distributed model, case 1,
V — averaged model, case 2,
VI — distributed model, case 2.

Table 1

%	I	II	III	IV	V	VI
CO	12.4	15.5	10.5	9.5	10	9.4
CO_2	24	22	23	18	23	18
H_2	59.4	59.8	53	49	52	48
CH_4	3.1	1.6	0.9	0.9	0.7	0.7

The results are not strictly comparable, because the model of the evolution of the active surface for coal particle is different here. Nevertheless, the agreement is quite satisfactory. Moreover, the present model makes it possible to simulate some additional phenomena like e.g. the start-up phase, the influence of the change in feed composition or temperature, and the transient states connected with them. A more sophisticated description of particle evolution may also be incorporated in the easy way.

Let us notice that both averaged and distributed models give similar numbers and the more complicated simulation reveals some additional details. Constructing such a consistent hierarchy of process descriptions is one of the ways of ensuring correctness of the simulation results.

Notation:

A — reactor crossection area, $[m^2]$
A_C — the active surface of particles per unit mass, $[m^2/kg]$
C_i^b, C_i^e — concentration of i-th gas in bubble an emulsion phases, $[kmol/m^3]$
D_i^b, D_i^e — gas diffusion coefficients in bubble and emulsion phases, $[m^2/s]$
E_i — activation energy for i-th reaction, $[kJ/kmol]$
F_{be} — gas exchange coeffeicient between bubble and emulsion phases, $[1/m]$
H — bed height, $[m]$
k_i — frequency factor i-th reaction, $[m/s]$ for gas-solid reaction, $[m^3/kmol \cdot s]$ for gas-gas reaction
M_C — a mol number of coal, 12 $[kg/kmol]$
$n\ (r,\ t)$ — normalised number of coal particles with radius r at the moment t
N_0 — normalising factor for $n\ (r,\ t)$
R — universal gas constant
R_i^b, R_i^e — rate of production for i-th gas in bubble and emulsion phases, $[kmol/m^3 \cdot s]$
R_C — rate of change for the mass of coal in bed, $[kg/s]$
S — the active surface of coal per unit volume of emulsion phase, $[1/m]$
T — bed temperature, $[K]$
$u^b \cdot u^e$ — gas flow velocity in bubble and emulsion phases, $[m/s]$
u_0 — velocity of incoming gas, $[m/s]$
u_{mf} — critical fluidization velocity, $[m/s]$
v — rate of shrinking for coal particles, $[m/s]$
W — bed mass, $[kg]$
W_C — mass of the coal in bed, $[kg]$
W_{in}, W_{out} — feeding and removal intensities, $[kg/s]$
δ — volume fraction of bubble phase
ε_{mf} — gas volume fraction in emulsion phase
ρ — density of coal, $[kg/m^3]$
$\overline{\rho}$ — average solid density in bed, $[kg/m^3]$

References

[1] Aerts J. Modelowanie procesu zgazowania węgla w zadanych warunkach termodynamicznych i kinetycznych. Internal report. Zakład Inżynierii Chemicznej i Konstrukcji Aparatury PAN, Gliwice 1983.

[2] Alekseyev B.V., Grishin A.M. Fizicheskaya gazodinamika reagiruyuschih sred. Moskwa, Vysshaya Shkola 1983.

[3] Buzek L., Kulawska M. Model fizykochemiczny autotermicznego parowotlenowego procesu zgazowania węgla w reaktorze fluidalnym. *Koks — Smola — Gaz*, **29** (1984) 12.

[4] Cooper D.J., Clough D.E. Real time estimation of dynamic particlesize distribution in a fluidized bed — theorethical foundations. *AIChEJ*, **31** (1985).

[5] Cooper D.J., Clough D.E. Optimal real-time monitoring of particlesize distribution in fluidized bed. *AIChEJ*, **32** (1986).
[6] Glowinsky R. Numerical methods for nonlinear variational problems. Springer 1984.
[7] Neogi D., Chang C.C., Walawender W.P., Fan L.T. Study of coal gasification in an experimental fluidized bed reactor. *AIChEJ*, **32** (1986).
[8] Niezgódka M., Żochowski A. A phenomenological model of gas-solid reactions for populations of particles with intrinsic dynamics. Control and Cybernetics, to appear.
[9] La Nauze R.D. Fundamentals of coal combustion in fluidized beds. *Chem. Eng. Res. Design*, **63** (1985).
[10] Sotirchas S.V., Amundson N.R. Dynamic behaviour of porous char particles in oxygen containing environment. *AIChEJ*, **30** (1984).
[11] Stetter H.J. Analysis of discretisation methods for ordinary differential equations. Springer 1973.
[12] Szekely J., Evans J.W., Sohn H.Y. Gas-solid reactions. New York, Academic Press 1976.
[13] Weimer A.W., Clough D.E. Modelling a low pressure steam-oxygen fluidized bed coal gasifying reactor. *Chem. Eng. Sci.*, **36** (1981).

Received, July 1988.

Modelowanie matematyczne reakcji gaz-ciało stałe w przypadku zgazowania węgla w złożu fluidalnym

Ogólny model reakcji gaz-ciało stałe przedstawiony w [8] zastosowano do procesu zgazowania węgla w złożu fluidalnym. Zaprezentowano schematy numeryczne i wyniki obliczeń dla modeli uśrednionego isotermicznego i rozłożonego isotermicznego. Wyniki porównano z pomiarami laboratoryjnymi zamieszczonymi w [7].

Математическое моделирование реакции газ-твердое тело в случае газификации угля в кипящем слое

Представленная в [8] общая модель реакции газ-твердое тело применяется для описания процесса газификации угля в кипящем слое. Представлены численные алгоритмы и результаты вычислений для усредненной изотермической и распределенной изотермической моделей. Результаты сравниваются с лабораторными измерениями, представленными в [7].